

Quantum spin glasses with cubic anisotropy

Z. Domański, T. K. Kopec*, and F. Pázmándi

Institute of Theoretical Physics, University of Lausanne, CH-1015 Lausanne, Switzerland

(Received 4 May 1993; revised manuscript received 6 October 1993)

An infinite-range quantum Ising spin glass with cubic anisotropy (K) is studied using the imaginary-time representation with the n -replica approach and the thermo-field dynamic method. Mean-field-theory phase diagrams in the temperature-anisotropy plane (T, K) for quantum spins S ranging from 2 to $9/2$ are presented. For integer-spin values and large cubic anisotropy (positive or negative, depending on S) a condensation into a nonmagnetic spin state occurs, accompanied by the destruction of the spin-glass order as indicated by the finite critical value $K_c(T=0)$. For half-integer S and sufficiently low temperature the spin-glass phase persists for arbitrary K .

I. INTRODUCTION

Cubic anisotropy plays an important role in systems with different types of interactions. Examples are orientational glasses¹ [such as the mixed crystal² $K(\text{Br})_x(\text{CN})_{1-x}$], ferroelectrically ordered perovskite-type compounds^{3,4} [such as $\text{KTa}_x\text{Nb}_{1-x}\text{O}_3$ (KTN) or BaTiO_3], or the ferromagnetic⁴ TbP. An isotropic orientational glass does not have a glass phase in three dimensions at nonzero temperature but this phase is stabilized by cubic anisotropy.⁵ Ferromagnets with single-ion cubic interaction can exhibit a particular type of critical behavior associated with the cubic fixed point of the renormalization-group transformation.⁶

Anisotropy has a profound influence on the spin-glass phase. For instance, strong uniaxial anisotropy of the magnetic susceptibility was found experimentally in a number of hexagonal metallic spin-glass systems⁷⁻⁹ and this has stimulated theoretical research. From a theoretical point of view, anisotropy gives rise to several new features which have been investigated for classical spin models both with and without a magnetic field, and a multiplicity of phases has been found.^{10,11}

The vector-spin-glass Hamiltonian with a cubic single-ion anisotropy term may be a relevant model for a number of spin-glass systems.¹ In the present paper we look at the effect of this single-ion cubic anisotropy which may be expected to be present if the material possesses one of the cubic structures. We include this anisotropy in the infinite-range Sherrington-Kirkpatrick (SK) model¹² as has been suggested by several authors.^{1,13}

Our paper is motivated by the conspicuous absence of study of the effects of cubic anisotropy on spin glasses. To our knowledge this problem has not been treated theoretically in the literature, except by Roberts¹⁴ (who investigated the metastable states of a classical spin glass with cubic anisotropy at $T=0$), although experimentally studied insulating compounds of the magnetic dilution series $\text{Eu}_x\text{Sr}_{1-x}\text{S}$ reveal spin-glass behavior in the presence of cubic symmetry.^{1,13,15}

For simplicity, we consider in detail the properties of an Ising-like model with random exchange interactions

and cubic anisotropy. Specifically, we consider the quantum version of the model, analyzing several cases corresponding to the spin values from $S=2$ to $S=9/2$ and presenting calculations of the phase diagrams.

In general, the quantum spin-glass problem is far from being trivial due to the noncommutativity of the operators involved, and different methods have been developed to handle it.¹⁶⁻¹⁹ Typically, quantum mechanics introduces time-dependent self-interactions and order parameters, complicating the problem considerably. In the present paper we adopt two different approaches to deal with both randomness and quantum features. The first approach relies on the replica method combined with the Matsubara "imaginary-time" representation for quantum operators.¹⁶ The second one is based on the thermofield dynamic (TFD)¹⁸ method, a real-time finite-temperature quantum field theory, which has been applied to a number of quantum systems.^{11,19,20}

The Hamiltonian of the model is given by

$$H = -\frac{1}{2} \sum_{i,j=1}^N J_{ij} S_{zi} S_{zj} + \sum_{i=1}^N H_{0i}, \quad (1)$$

where $\mathbf{S}_i = (S_{xi}, S_{yi}, S_{zi})$ is the quantum spin operator associated with the local moment S at site $i = 1, \dots, N$. The random exchange interactions J_{ij} ($i \neq j$) are governed by independent probability distributions, each taken to be Gaussian with zero mean and variance J/\sqrt{N} . The second term in Eq. (1) is given by

$$H_{0i} = -K(S_{xi}^4 + S_{yi}^4 + S_{zi}^4) \quad (2)$$

and describes the cubic anisotropy favoring spin alignment along the edges ($K > 0$) or diagonals ($K < 0$) of a three-dimensional cube with edges along the respective coordinate axes.

II. IMAGINARY-TIME REPLICA APPROACH

The derivation of the free energy, using the Matsubara time formalism, is a straightforward generalization of the

work of Bray and Moore.¹⁶ In order to average over the random couplings $\{J_{ij}\}$ we apply the replica method and the Matsubara “time” representation, which allows us to treat the noncommuting spin operators as c numbers. Within the replica-symmetric theory for the free energy per spin one obtains

$$f[R] = q^2 - \int_0^1 d\tau \int_0^1 d\tau' R^2(\tau, \tau') + \int_{-\infty}^{+\infty} \frac{d\xi}{\sqrt{2\pi}} e^{-\xi^2/2} \ln \Theta_\xi[R, q], \quad (3)$$

where

$$\begin{aligned} \Theta_\xi[R, q] &= \text{Tr} \exp(-\beta H_0) T_\tau \exp\{\xi \sqrt{2\beta J q} I(S_z) - q(\beta J)^2 I^2(S_z) + \Phi[R]\}, \\ \Phi[R] &= \beta J \int_0^1 d\tau \int_0^1 d\tau' R(\tau, \tau') S_z(\tau) S_z(\tau'), \\ I(S_z) &= \int_0^1 d\tau S_z(\tau), \\ S_z(\tau) &= \exp(-\tau \beta H_0) S_z \exp(\tau \beta H_0), \quad \text{and} \quad \beta = 1/kT. \end{aligned} \quad (4)$$

Here, T_τ denotes the “time”-ordering operator which rearranges the operators in the expansion of the exponential, in order of decreasing “time” arguments τ . The quantity q corresponds to the Edwards-Anderson²¹ spin-glass order parameter and $R(\tau, \tau')$ is the dynamic spin self-interaction. Both quantities should be determined self-consistently.

In the paramagnetic phase q vanishes and the phase transition takes place when the coefficient of q^2 in the free energy expansion as a function of the temperature T becomes zero. Thus, the spin freezing temperature can be evaluated directly from an expression calculated in the high-temperature phase. The equation of the phase transition line becomes

$$1 = 2 \int_0^1 d\tau \int_0^1 d\tau' R(\tau, \tau'). \quad (5)$$

The dynamic self-interaction (determined via the saddle-point evaluation) is given by the self-consistent equation

$$R(\tau, \tau') = (\beta J/2) \langle S_z(\tau) S_z(\tau') \rangle_{\text{eff}}. \quad (6)$$

Here, the angular brackets mean the thermal average with respect to the effective Hamiltonian defined in the exponent of Eq. (4) with $q = 0$. Since the exact resolution of Eq. (6) is not yet available due to the difficulties associated with the imaginary-time dependence of the dynamic spin self-interaction, we are forced to resort to some approximations. We employ the so-called static approximation (SA) where the time dependence of R is neglected, i.e.,

$$R(\tau, \tau') = R_0. \quad (7)$$

As a result the free energy per spin becomes

$$f_{\text{SA}} = -R_0^2 + \ln \int_{-\infty}^{+\infty} \frac{d\xi}{\sqrt{2\pi}} e^{-\xi^2/2} \text{Tr} \exp(H_{\text{eff}}^{\text{SA}}), \quad (8)$$

where

$$H_{\text{eff}}^{\text{SA}} = \beta K (S_x^4 + S_y^4 + S_z^4) + \xi \sqrt{2\beta J R_0} S_z. \quad (9)$$

Finally, from Eq. (8), the formula for the critical line is

found to be

$$\int_{-\infty}^{+\infty} \frac{d\xi}{\sqrt{2\pi}} e^{-\xi^2/2} (\xi^2 - 2) \text{Tr} \exp(H_{\text{eff}}^{\text{SA}}) = 0, \quad (10)$$

where the trace can be calculated by using the eigenvalues of $H_{\text{eff}}^{\text{SA}}$ given in Appendix A. For example, for $S = 2$ the phase boundary in the temperature-anisotropy plane is given by

$$\begin{aligned} \int_{-\infty}^{+\infty} \frac{d\xi}{\sqrt{2\pi}} e^{-\xi^2/2} (\xi^2 - 2) \cosh \left[\sqrt{(3\beta K)^2 + 4\beta J \xi^2} \right] \\ = \frac{1}{2} e^{3\beta K} + (1 - \beta J) e^{\beta(J/2 - 3K)}. \end{aligned} \quad (11)$$

The corresponding phase diagram is presented in Fig. 1.

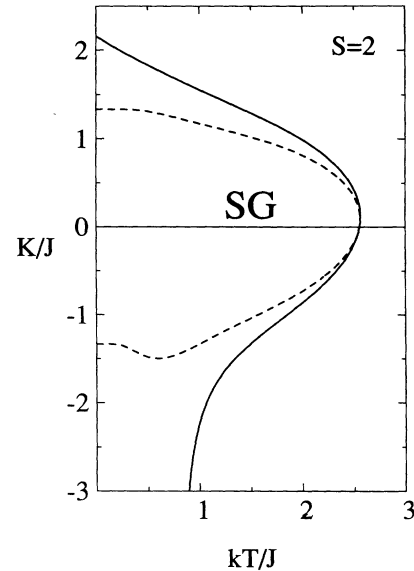


FIG. 1. The anisotropy-temperature phase diagram for $S = 2$; solid curve, static approximation (SA); dashed curve, thermofield dynamic (TFD) method. The lines separate the spin-glass (SG) phase from the paramagnetic region. K , anisotropy constant as defined in Eq. (2); $J = (\langle J_{ij}^2 \rangle N)^{1/2}$; T , temperature; k , Boltzmann's constant.

For other values of S the critical $K_c(T)$ lines are given in Figs. 2–6. Two types of phase separation curves are found. The first type reaches the line $kT/J = 0$ (as, e.g., in Fig. 1 for $K/J > 0$) whereas the second one approaches a vertical asymptote $kT/J > 0$ in the limit as $|K|/J \rightarrow \infty$ (as, e.g., in Fig. 1 for $K/J < 0$). Hereafter the critical behavior associated with the latter type of the phase separation line is called the asymptotic behavior. The critical behavior in the limiting cases, $K/J \rightarrow \pm\infty$, is investigated in Appendix A.

We can test our results by comparing them with exact results available for the cases $K = 0$ and $|K|/J \rightarrow \infty$. The case $K = 0$ corresponds to the classical Ising SK model for which the exact critical temperature T_c as a function of S is given by

$$1 = 2u \frac{\partial}{\partial u} \ln \text{Tr} \exp(uS_z^2), \quad (12)$$

$$\frac{kT_c}{J} = \frac{1}{2u}.$$

For all spins considered this T_c is recovered by the SA, as it should be because the static approximation is exact for the classical Ising SK model.

In order to analyze the large anisotropy limits $K/J \rightarrow \pm\infty$ we apply perturbation theory²² considering the SK Hamiltonian of Eq. (1) as a perturbation. The effective Hamiltonian $H_{\text{eff}} = \hat{P}H\hat{P}$ acts on the Hilbert space \mathcal{H}_{min} associated with the ground state energy of H_0 [Eq. (2)] and \hat{P} is a projection operator onto \mathcal{H}_{min} . The resulting H_{eff} is

$$H_{\text{eff}} = -\frac{1}{2} \sum_{i,j} J_{ij} S_{zi}^{\text{eff}} S_{zj}^{\text{eff}}, \quad (13)$$

with an effective spin $S_z^{\text{eff}} = \hat{P}S_z\hat{P}$. Since the energy levels of H_0 are separated by gaps proportional to $|K|$, H_{eff} [Eq. (13)] becomes exact when $|K| \rightarrow \infty$.

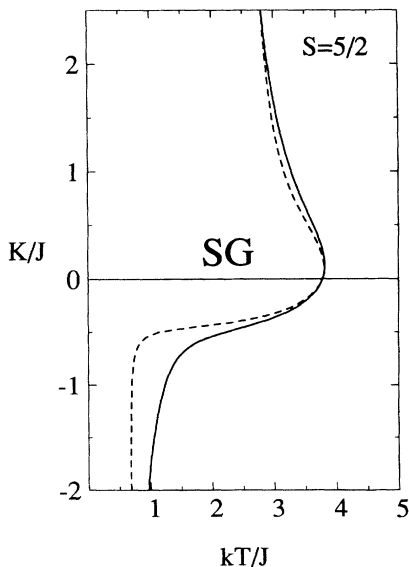


FIG. 2. The anisotropy-temperature phase diagram for $S = 5/2$. Notation as in Fig. 1.

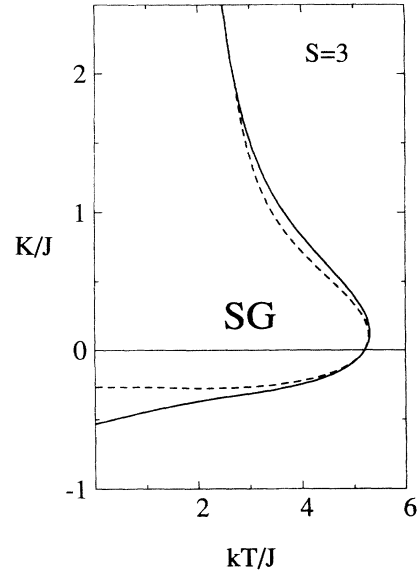


FIG. 3. The anisotropy-temperature phase diagram for $S = 3$. Notation as in Fig. 1.

The spectrum of the cubic anisotropy Hamiltonian (2) has been calculated²³ for $S = 2, \dots, 8$. For $S = 2$ it consists of a triplet (lowest for $K/J < 0$) and a doublet. The corresponding S_z^{eff} are

$$S_t = \begin{bmatrix} 1 & 0 & 0 \\ 0 & 0 & 0 \\ 0 & 0 & -1 \end{bmatrix} \quad \text{and} \quad S_d = \begin{bmatrix} 0 & 0 \\ 0 & 0 \end{bmatrix} \quad (14)$$

in the limits $K/J \rightarrow -\infty$ and $K/J \rightarrow \infty$, respectively. For negative anisotropy the resulting temperature $kT_c/J = 0.79$ [Eq. (12)] gives the asymptotic behavior of the original system presented in Fig. 1 [see Eq. (A1)]. In

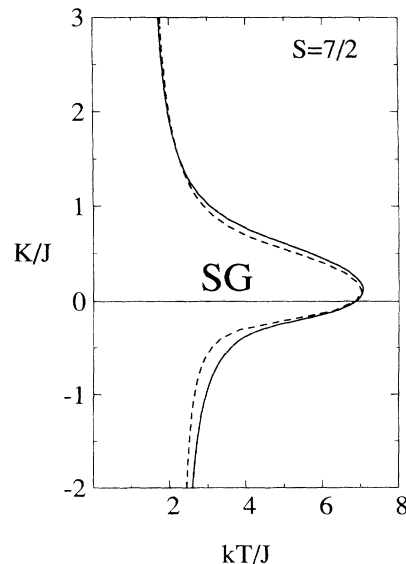


FIG. 4. The anisotropy-temperature phase diagram for $S = 7/2$. Notation as in Fig. 1.

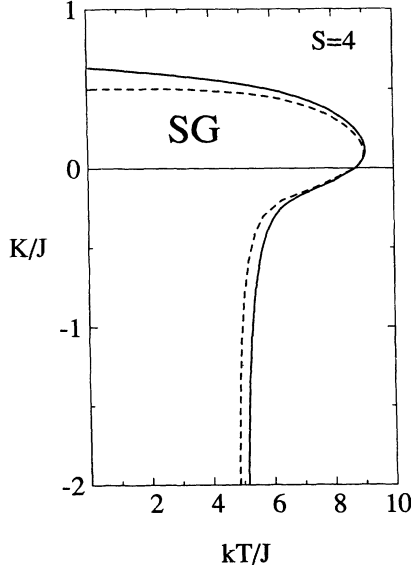


FIG. 5. The anisotropy-temperature phase diagram for $S = 4$. Notation as in Fig. 1. The reduced temperature for the asymptotic behavior ($K/J \rightarrow -\infty$) from the SA method is $kT_c/J = 4.94$, and from the TFD method is $kT_c/J = 4.71$.

the opposite limit ($K/J \rightarrow \infty$) the effective spin yields a paramagnetic state for arbitrary T . Since for $K = 0$ and $kT/J < 2.553$ there is a spin-glass order, there should be a finite $K_c(T = 0)$ at which the transition between the spin-glass phase and paramagnetic phase occurs. The SA estimates this critical anisotropy strength as $2.15J$. The cases $S = 5/2, 3, \dots, 9/2$ are discussed in Appendix B. For all spins the SA predictions are consistent with the large anisotropy analysis.

III. THERMOFIELD DYNAMIC METHOD

A detailed procedure for applying the TFD method to spin-glass models has been described in Ref. 19. Here we sketch this approach giving only those points necessary to explain the position of the phase transition line. We start

$$\begin{aligned} \text{Tr} \mathbf{Q}^2 &= \int_{-\infty}^{+\infty} dt \int_{-\infty}^{+\infty} dt' \sum_{ab} Q^{ab}(t, t') Q^{ba}(t', t), \\ \Phi[\mathbf{Q}] &= \langle O, \beta | T_t \exp \left(-i \int_{-\infty}^{+\infty} dt \int_{-\infty}^{+\infty} dt' \hat{H}_Q(t, t') \right) | O, \beta \rangle, \end{aligned}$$

and $\langle O, \beta | \dots | O, \beta \rangle = \text{Tr} \exp(-\beta H_0) \dots / \text{Tr} \exp(-\beta H_0)$. Here, the time-ordered exponential results from the interaction picture, and $Q^{ab}(t, t') = Q^{ba}(t', t)$ represents a symmetric time-dependent tensor field. The effective time-dependent single-site thermal Hamiltonian is given by

$$\hat{H}_Q(t, t') = - \sum_{ab} (\epsilon_a \epsilon_b)^{1/2} J Q^{ab}(t, t') S_z^a(t) S_z^b(t'), \quad (17)$$

where $a, b = 1, 2$ are the TFD “dynamic replicas” ($\epsilon_1 = 1, \epsilon_2 = -1$) labeling the collective fields JQ^{ab} which act as dynamic self-interactions between time-dependent spin operators $S_z^a(t) = \exp(-iH_0 t) S_z^a \exp(iH_0 t)$. From Eq. (17) it

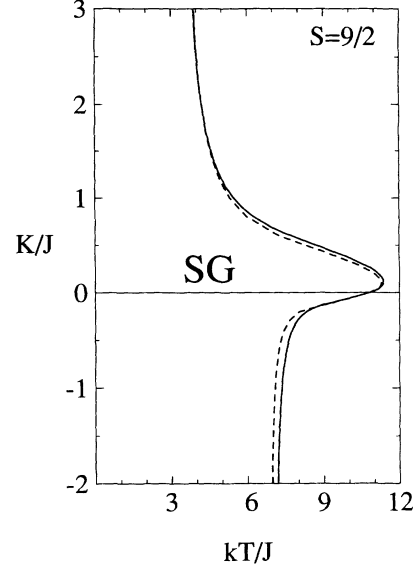


FIG. 6. The anisotropy-temperature phase diagram for $S = 9/2$. Notation as in Fig. 1. The reduced temperatures obtained for the asymptotic behavior from the SA and TFD methods coincide for $K/J \rightarrow \infty$ and $kT_c/J = 3.55$. For the opposite limit $kT_c/J = 7$ from the SA method, and $kT_c/J = 6.88$ from the TFD method.

from the disorder-averaged generating functional for the real-time finite-temperature causal Green’s functions in the form

$$\langle Z[\eta, \{J_{ij}\}] \rangle_J = \int \prod_{ab} DQ^{ab} \exp(-NL[\mathbf{Q}] + \Omega[\eta]), \quad (15)$$

where $Z[\eta, \{J_{ij}\}]$ is the unaveraged generating functional for a fixed realization of random bonds and $\Omega[\eta] = \text{Tr}(\mathbf{Q}\eta)/J^2$ represents the source term. In the interaction picture with respect to the single-body Hamiltonian (2) the single-site dynamic effective Lagrangian is

$$L[\mathbf{Q}] = \text{Tr} \mathbf{Q}^2 - \ln \Phi[\mathbf{Q}], \quad (16)$$

where

can be seen that the quantum generalization of the problem results in a time-dependent self-interaction $JQ^{ab}(t, t')$ between spin operators at the same site, which must be determined self-consistently. In the limit $N \rightarrow \infty$ the steepest descent method can be used giving the following equation for the stationary-point value of the dynamic self-interaction:

$$Q_0^{ab}(t, t') = \frac{1}{2}(\epsilon_a \epsilon_b)^{1/2} JG^{ab}(t, t'), \quad (18)$$

where the causal Green's function is defined as

$$G^{ab}(t, t') = -i \frac{\langle O, \beta | T_t S_z^a(t) S_z^b(t') U_{Q_0}(-\infty; +\infty) | O, \beta \rangle}{\langle O, \beta | T_t U_{Q_0}(-\infty; +\infty) | O, \beta \rangle}. \quad (19)$$

The correspondence with measurable quantities is achieved by the following decomposition of the Fourier transformed G^{ab} :

$$G^{ab}(\omega) = [\mathbf{U}_B(\omega) \hat{\tau} \bar{G}(\omega) \mathbf{U}_B(\omega)]^{ab},$$

where $\mathbf{U}_B(\omega)$ is the thermal transformation matrix,²⁴ while $\bar{G}^{ab}(\omega)$ is the matrix of retarded (advanced) $G_{R(A)}(\omega)$ Green's functions,

$$\bar{G}^{ab}(\omega) = \begin{pmatrix} G_R(\omega) & 0 \\ 0 & G_A(\omega) \end{pmatrix} \quad \text{and} \quad \hat{\tau} = \begin{pmatrix} 1 & 0 \\ 0 & -1 \end{pmatrix}. \quad (20)$$

To locate the temperature-anisotropy critical line one observes that the generalized damping function

$$\gamma^{-1}(\omega) = i \frac{\partial G_R^{-1}(\omega)}{\partial \omega} \quad (21)$$

diverges in the static limit ($\omega \rightarrow 0$) along the line $K_c(T)$. The dynamic response function $G_R(\omega)$ itself obeys the Dyson equation

$$G_R(\omega) = \frac{\Sigma_R(\omega)}{1 - JG_R(\omega)}, \quad (22)$$

where $\Sigma_R(\omega)$ denotes the self-energy part. Differentiation of Eq. (22) with respect to ω leads to

$$\gamma^{-1}(\omega) = i \frac{\partial \Sigma_R^{-1}(\omega) / \partial \omega}{1 - J^2 G_R^2(\omega)}. \quad (23)$$

The condition for divergence of the damping function $\gamma^{-1}(\omega)$ is

$$1 = J\chi, \quad (24)$$

where

$$\chi = \lim_{\omega \rightarrow 0} G_R(\omega) = \lim_{\omega \rightarrow 0} G_A(\omega). \quad (25)$$

Because of the appearance of the dynamic self-interaction $JQ^{ab}(\omega)$ in the effective thermal Hamiltonian (17), the explicit resolution of Eq. (19) is rather a formidable task. For this reason we focus on the ef-

fects of quantum fluctuations on a time scale such that the finite-time part of the dynamic self-interaction can be presented by an instantaneous term

$$Q^{ab}(t - t') = \frac{1}{2}(\epsilon_a \epsilon_b)^{1/2} J\chi \delta(t - t') \delta_{ab}. \quad (26)$$

It follows that

$$\chi = - \sum_{\ell=1}^{2S+1} \left\{ \left[\frac{\partial^2 \lambda_\ell(h)}{\partial h^2} \right]_{h=0} - \beta \left[\frac{\partial \lambda_\ell(h)}{\partial h} \right]_{h=0}^2 \right\} \rho_\ell, \quad (27)$$

where

$$\rho_\ell = \frac{\exp[-\beta \lambda_\ell(0)]}{\sum_{k=1}^{2S+1} \exp[-\beta \lambda_k(0)]}. \quad (28)$$

Here, $\lambda_\ell(h)$ ($\ell = 1, \dots, 2S + 1$) represents an eigenvalue of the effective single-site quantum spin Hamiltonian of the instantaneous approximation (IA) [Eq. (26)]

$$H_{\text{eff}}^{\text{IA}} = -\frac{1}{2} J^2 \chi (S_z)^2 - K (S_x^4 + S_y^4 + S_z^4). \quad (29)$$

These eigenvalues have been calculated (see Appendix A).

The critical line equation for $S = 2$ is $1 = J\chi$ [Eq. (24)], where the static susceptibility is given by

$$\chi = \frac{8 \exp(3\beta K + 2\beta \chi J^2) \sinh(3\beta |K|) + 6\beta \exp(\beta \chi J^2/2) |K|}{6 \exp(3\beta K + 2\beta \chi J^2) |K| \cosh(3\beta |K|) + [3 \exp(6\beta K) + 6 \exp(\beta \chi J^2/2)] |K|}. \quad (30)$$

The corresponding phase diagram is presented in Fig. 1. For the remaining values of S the critical lines $K_c(T)$ are presented in Figs. 2–6 and the asymptotic behavior $K/J \rightarrow \pm\infty$ is considered in Appendix A. In the limit $K \rightarrow 0$ the IA yields the exact critical temperature $T_c(K=0)$ [Eq. (12)] for all spins. A qualitative difference between the large anisotropy analysis and the IA is found only for $S=2$. For $K < 0$ the IA predicts the phase transition at finite $K_c(T=0)$ whereas the former method and the SA yield an asymptotic behavior. We do not know at present why this difference occurs.

IV. SUMMARY

Cubic anisotropy leads to a strong modification of the phase diagram of a spin-glass model. The cases of integer and half-integer S are quite different. In the systems with integer spin for large negative or positive anisotropy K (depending on S), a condensation into the nonmagnetic state results, accompanied by the destruction of the spin-glass order indicated by the finite critical value K_c as the temperature approaches zero. We have shown that this behavior results from a nonmagnetic ground state of the anisotropy Hamiltonian (2), occurring for integer S . This state becomes the ground state of the whole system in the large anisotropy limit. For half-integer spin we observe an asymptotic behavior for negative and positive values of K . Since the same type of phase diagram results also from the Hamiltonian (1) in which the random interactions are replaced by ferromagnetic short-range interactions,²⁵ it is clear that the anisotropy energy is very important. In all cases, in the vicinity of T_c for small $K > 0$, there is a temperature region with a reentrant behavior in the temperature-anisotropy phase diagram. In this case, as the anisotropy is lowered, the system passes from the paramagnetic (P) phase to the spin-glass (SG) state, and, by further lowering the anisotropy, the system reenters the paramagnetic region. Similar reentrance was observed experimentally in rare-earth spin glasses with uniaxial anisotropy⁸ and reported in several theoretical papers dealing with the quantum version of the model.^{11,26,27} Generally, such a type of $P-SG-P$ reentrance was predicted theoretically²⁸ to be present in randomly mixed magnets at dimensionalities $d > 6$. It is interesting to note that the character of the phase diagrams of the systems with cubic single-ion anisotropy is like that due to the presence of uniaxial anisotropy. In the systems with integer spins, uniaxial anisotropy also leads to the destruction of magnetic order in the presence of both the long-range (random²⁶) as well as the short-range (antiferromagnetic²⁹) interactions.

For the quantum spin-glass problem an exact calculation of the transition lines requires precise knowledge of the time dependence of the dynamic spin self-interaction involved. This means that the calculation of the exact phase boundary will depend on the detailed time dependence of $Q^{ab}(t)$ (in the TFD method) and of $R(\tau)$ (in the Matsubara approach with the replica method). It seems

that the complexity of the problem prevents an analytically tractable approach which goes beyond the *Ansätze* (7) and (26). A difference between the Matsubara imaginary-time static approximation and the thermo-field dynamics instantaneous real-time approximation is found for the case $S=2$, where, for large negative anisotropy K , the former method predicts asymptotic behavior, whereas the latter yields a finite critical value $K_c(T=0)$. The investigation of this $S=2$ case using methods along the lines given in Ref. 30 is currently under way. As was pointed out earlier,³¹ the static and instantaneous approximations will give rough upper and lower bounds, respectively, for the critical line $K_c(T)$. In conclusion, the exact phase boundary should be located in the region between two curves corresponding to the above-mentioned approximations. It is interesting to note that for $S > 2$ the phase boundaries determined by both methods are closer together as S increases.

We expect a similarly rich behavior for other models with cubic anisotropy, e.g., the XY or Heisenberg systems, where the presence of additional vector spin components will give rise to a multitude of spin-glass phases, such as transverse or longitudinal phases. A precise calculation of phase boundary lines, especially of those separating different spin-glass orderings (i.e., in the non-ergodic regions), would presumably require a quantum analog of the replica-symmetry breaking scheme. An extension of this work covering the above-mentioned issues is under investigation.

ACKNOWLEDGMENTS

The support of the Swiss National Science Foundation through Grant No. 20-28846.90 and of the Foundation Herbetta is gratefully acknowledged. The authors thank Paul Erdős for helpful discussions and the critical reading of the manuscript. One of the authors (T.K.K.) thanks the members of the Institute of Theoretical Physics of the University of Lausanne for their warm hospitality.

APPENDIX A

The listing of the eigenvalues corresponding to the effective single-site Hamiltonian $H_{\text{eff}}^{\text{IA}}$ (29) is given below for several values of the spin quantum numbers S . For the eigenvalues relevant to $H_{\text{eff}}^{\text{SA}}$ (9) one has to substitute $\chi \rightarrow 0$, $h \rightarrow \xi\sqrt{2\beta R_0}$, and $K \rightarrow \beta K$, respectively.

1. $S=2$

$$\begin{aligned}\lambda_1(h) &= -24K, \\ \lambda_{2,3}(h) &= \frac{\pm 2h - \chi J^2}{2} - 18K, \\ \lambda_{4,5}(h) &= -2\chi J^2 - 21K \pm \sqrt{4h^2 + 9K^2}.\end{aligned}$$

The temperature for the asymptotic behavior ($K/J \rightarrow -\infty$) from the SA method is determined by

$$2\beta J \frac{\exp\left(\frac{1}{2}\beta J\right)}{1 + 2\exp\left(\frac{1}{2}\beta J\right)} = 1, \quad (\text{A1})$$

with $kT_c/J = 0.79$.

2. $S = 5/2$

$$\begin{aligned} \lambda_{1,2}(h) &= \frac{\pm 4h - \chi J^2}{8} - \frac{803K}{16}, \\ \lambda_{3,4}(h) &= \frac{-(8h + 34\chi J^2 + 659K)}{16} \\ &\quad \pm \sqrt{(9K^2 + \chi J^2 + 2h)^2 - 12K(\chi J^2 + h)}, \\ \lambda_{5,6}(h) &= \lambda_{3,4}(-h). \end{aligned}$$

The reduced temperature kT/J for the asymptotic behavior ($K/J \rightarrow -\infty$) obtained by the SA and TFD methods is $kT_c/J = 25/36$. For $K/J \rightarrow +\infty$ the SA gives

$$\left(\frac{\beta J}{36}\right) \frac{121 \exp\left(\frac{121}{72}\beta J\right) + 9 \exp\left(\frac{1}{8}\beta J\right)}{\exp\left(\frac{121}{72}\beta J\right) + \exp\left(\frac{1}{8}\beta J\right)} = 1,$$

which yields $kT_c/J = 2.31$. From the TFD method we have, in the limit $K/J \rightarrow +\infty$,

$$\left(\frac{\beta J}{36}\right) \frac{121 \exp\left(\frac{67}{24}\beta J\right) + 9 \exp\left(\frac{1}{8}\beta J\right)}{\exp\left(\frac{67}{24}\beta J\right) + \exp\left(\frac{1}{8}\beta J\right)} = 1,$$

giving $kT_c/J = 2.552$.

3. $S = 3$

$$\begin{aligned} \lambda_1(h) &= -102K, \\ \lambda_{2,3}(h) &= -2\chi J^2 - 63K \pm \sqrt{4h^2 + 225K^2}, \\ \lambda_{4,5}(h) &= \frac{-(2h + 5\chi J^2 + 180K)}{2} \\ &\quad \pm \sqrt{(6K + \chi J^2 + h)^2 - 9K(2\chi J^2 + h)}, \\ \lambda_{6,7}(h) &= \lambda_{4,5}(-h). \end{aligned}$$

The reduced temperature kT/J for the asymptotic behavior $K/J \rightarrow +\infty$ obtained by the SA method follows from the equation

$$\left(\frac{9}{2}\beta J\right) \frac{\exp\left(\frac{9}{8}\beta J\right)}{1 + \exp\left(\frac{9}{8}\beta J\right)} = 1,$$

with $kT_c/J = 1.78$, and from TFD method

$$\left(\frac{9}{2}\beta J\right) \frac{\exp(3\beta J)}{1 + 2\exp(3\beta J)} = 1,$$

with $kT_c/J = 2.02$.

4. $S = 7/2$

$$\begin{aligned} \lambda_{1,2}(h) &= \frac{-(8h + 34\chi J^2 + 1947K)}{16} \\ &\quad \pm \sqrt{(30K + \chi J^2 + 2h)^2 - 90K(\chi J^2 + h)}, \\ \lambda_{3,4}(h) &= \lambda_{1,2}(-h), \\ \lambda_{5,6}(h) &= \frac{-(24h + 50\chi J^2 + 2715K)}{16} \\ &\quad \pm \sqrt{(18K + 3\chi J^2 + 2h)^2 - 42K(3\chi J^2 + 2h)}, \\ \lambda_{7,8}(h) &= \lambda_{5,6}(-h). \end{aligned}$$

The reduced temperatures kT/J for the asymptotic behaviors ($K/J \rightarrow \pm\infty$) from the SA and TFD methods are respectively $kT_c/J = 49/36$ (for $K > 0$) and $kT_c/J = 9/4$ (for $K < 0$).

The expressions corresponding to the eigenvalues for $S = 4$ and $S = 9/2$ are given in terms of the roots of a cubic equation and are not reproduced here.

APPENDIX B

In the large anisotropy limit the cases $S = 3$ and $S = 4$ are similar to that of $S = 2$ where condensation onto the nonmagnetic state occurs. For $S = 3$ the eigenenergies of H_0 [Eq. (2)] form a singlet (lowest for $K/J < 0$) and two triplets. The respective forms of S_z^{eff} are given by [0] and $3/2S_t$ [see Eq. (14)]. Thus, the paramagnetic–spin-glass transition occurs for finite negative K_c/J , whereas in the limit $K/J \rightarrow \infty$ the asymptotic behavior is characterized by $kT_c/J = 1.78$ (see Fig. 3).

In the case $S = 4$ we have the lowest triplet for $K/J \rightarrow -\infty$ and a singlet ground state for the opposite limit. The corresponding S_z^{eff} have the following forms: $5/2S_t$ and [0]. In the limit $K/J \rightarrow \infty$, we have the paramagnetic state, with the paramagnetic–spin-glass transition at $T = 0$. The opposite anisotropy limit yields the asymptotic character with $kT_c/J = 4.94$ (Fig. 5).

All systems with half-integer spins that we studied reveal a spin-glass order at low temperature in both the limits ($K/J \rightarrow \pm\infty$). For $S = 5/2$ the spectrum of H_0 [Eq. (2)] is a doublet and a quartet (lowest for $K/J > 0$) with the respective S_z^{eff} operators $5/6\sigma_z$ (σ_z is a Pauli spin matrix) and a diagonal operator with a diagonal: $\{11/6, 1/2, -1/2, -11/6\}$. The resulting kT_c/J are respectively equal to $25/36$ ($K/J \rightarrow -\infty$) and 2.31 ($K/J \rightarrow \infty$). For $S = 7/2$ in both the limits ($K/J \rightarrow \pm\infty$) the lowest energy level is doubly degenerate. The resulting S_z^{eff} operators have the forms $3/2\sigma_z$ and $7/6\sigma_z$ for the $-\infty$ and ∞ limits, respectively. The resulting kT_c/J are $9/4$ and $49/36$ (see Fig. 4). A similar analysis for $S = 9/2$ yields the asymptotic behavior characterized by $kT_c/J = 121/36$ ($K/J \rightarrow \infty$) and $kT_c/J = 7$ ($K/J \rightarrow -\infty$) as shown in Fig. 6.

- * Permanent Address: Institute for Low Temperature and Structure Research, Polish Academy of Sciences, P.O. Box 937, 50-950 Wrocław 2, Poland.
- ¹ K. Binder and J. D. Reger, *Adv. Phys.* **41**, 547 (1992).
- ² K. Knorr, *Physica Scr. T* **19**, 531 (1987); J. M. Rowe and J. J. Rush, *Phys. Rev. Lett.* **43**, 1158 (1979).
- ³ M. Kerszberg and D. Mukamel, *Phys. Rev. B* **23**, 3943 (1981).
- ⁴ D. Blankschtein and A. Aharony, *Phys. Rev. Lett.* **47**, 439 (1981); *Phys. Rev. B* **28**, 386 (1983).
- ⁵ H.-O. Carmesin, *J. Phys. A* **22**, 297 (1989).
- ⁶ A. Aharony, in *Phase Transitions and Critical Phenomena*, edited by C. Domb and M. S. Green (Academic, New York, 1976), Vol. 6, p. 357.
- ⁷ H. Albrecht, E. F. Wassermann, F. T. Hedgcock, and P. Monod, *Phys. Rev. Lett.* **48**, 819 (1982); A. Fert, P. Pureur, F. Hippert, K. Baberschke, and F. Bruss, *Phys. Rev. B* **26**, 5300 (1982); S. Murayama, K. Yokosawa, Y. Miyako, and E. F. Wassermann, *Phys. Rev. Lett.* **57**, 1785 (1986).
- ⁸ K. Baberschke, P. Pureur, A. Fert, R. Wendler, and S. Senoussi, *Phys. Rev. B* **29**, 4999 (1984).
- ⁹ K. H. Fischer and J. A. Hertz, *Spin Glasses* (Cambridge University Press, Cambridge, England, 1991).
- ¹⁰ D. J. Elderfield and D. Sherrington, *J. Phys. A* **15**, L437 (1982); *J. Phys. C* **16**, 4865 (1983); D. M. Cragg, D. Sherrington, and M. Gabay, *Phys. Rev. Lett.* **49**, 158 (1982).
- ¹¹ T. K. Kopeć, G. Büttner, and K. D. Usadel, *Phys. Rev. B* **41**, 9221 (1990).
- ¹² D. Sherrington and S. Kirkpatrick, *Phys. Rev. Lett.* **35**, 1972 (1975).
- ¹³ H. Maletta and P. Convert, *Phys. Rev. Lett.* **42**, 108 (1979).
- ¹⁴ S. A. Roberts, *J. Phys. C* **15**, 4155 (1982).
- ¹⁵ H. Maletta, *J. (Paris) Colloq.* **41**, C5-115 (1980).
- ¹⁶ A. J. Bray and M. A. Moore, *J. Phys. C* **13**, L655 (1980).
- ¹⁷ M. Suzuki, *Prog. Theor. Phys.* **56**, 1454 (1976); *Phys. Rev. B* **31**, 2957 (1985); T. Yamamoto and H. Ishii, *J. Phys. C* **20**, 6053 (1987); L. De Cesare, K. Lukierska-Walasek, I. Rabuffo, and K. Walasek, *Phys. Rev. B* **45**, 1041 (1992).
- ¹⁸ H. Umezawa, H. Matsumoto, and M. Tachiki, *Thermo Field Dynamics and Condensed States* (North-Holland, Amsterdam, 1982).
- ¹⁹ T. K. Kopeć, *J. Phys. C* **21**, 297 (1988); **21**, 6053 (1988); T. K. Kopeć and G. Büttner, *Phys. Rev. B* **43**, 10 853 (1991).
- ²⁰ T. K. Kopeć and H. Umezawa, *Phys. Rev. B* **47**, 8923 (1993); T. K. Kopeć, *ibid.* **48**, 3698 (1993).
- ²¹ S. F. Edwards and P. W. Anderson, *J. Phys. F* **5**, 965 (1975).
- ²² P. Fulde, *Electron Correlations in Molecules and Solids* (Springer-Verlag, Berlin, 1991).
- ²³ K. R. Lea, M. J. M. Leask, and W. P. Wolf, *J. Phys. Chem. Solids* **23**, 1381 (1962).
- ²⁴ H. Matsumoto, Y. Nakano, and H. Umezawa, *J. Math. Phys.* **25**, 3076 (1984).
- ²⁵ Z. Domański and J. Sznajd, *Phys. Status Solidi B* **129**, 135 (1985); A. I. Mitsek, K. Yu. Guslienko, and S. V. Pavlovskii, *ibid.* **135**, 173 (1986).
- ²⁶ K. D. Usadel, K. Bien, and H.-J. Sommers, *Phys. Rev. B* **27**, 6957 (1983).
- ²⁷ G. Büttner and K. D. Usadel, *Europhys. Lett.* **14**, 165 (1991).
- ²⁸ S. Fishman and A. Aharony, *Phys. Rev. B* **21**, 280 (1980).
- ²⁹ T. Moriya, *Phys. Rev.* **117**, 635 (1960).
- ³⁰ F. Pázmándi, Z. Domański, and P. Erdős, *Phys. Rev. B* **47**, 8285 (1993); F. Pázmándi and Z. Domański, *J. Phys. Condens. Matter* **5**, L117 (1993).
- ³¹ K. D. Usadel, G. Büttner, and T. K. Kopeć, *Phys. Rev. B* **44**, 12 583 (1991).